

CONF 001984 9

CONF-890902--19

DE90 001984

12. REFLECTION ASYMMETRIC SHAPES IN NUCLEI

I. Ahmad, M. P. Carpenter, H. Emling,* R. Holzmann,* R. V. F. Janssens, T. L. Khoo, E. F. Moore, L. R. Morss, Argonne National Laboratory, Argonne, Illinois 60439, J. L. Durell, J. B. Fitzgerald, A. S. Mowbary, M. A. Hotchkiss, and W. R. Phillips, Department of Physics, University of Manchester, Manchester M13 9PL, England, M. W. Drigert, INEL, EG&G Idaho Inc., Idaho Falls, Idaho 83415, D. Ye, University of Notre Dame, Notre Dame, Indiana 46556 and Ph. Benet Purdue University, West Lafayette, Indiana 47907

* Present address: GSI, Planckstrasse 1, D-6100, Darmstadt, West Germany.

12.1 INTRODUCTION

Soon after the collective nuclear model [1,2] was established, low-lying negative parity states were observed [3] in even-even Ra and Th nuclei from alpha-particle spectroscopic studies. These negative parity levels formed a rotational band with spin sequence 1, 3, 5, and K quantum number 0. Since these states had energies much lower than the expected two quasi-particle states, these were interpreted as octupole vibrations about a spheroidal equilibrium shape. Ever since the discovery of the octupole vibrations, scientists have been thinking about the possibility of octupole deformations in nuclei, that is, nuclei with octupole equilibrium shape. These octupole shapes are symmetric about the Z axis but reflection asymmetric about the XY plane and resemble a pear.

END OF THIS DOCUMENT IS ENCL. 2B

The submitted manuscript has been authored by a contractor of the U. S. Government under contract No. W-31-109-ENG-38. Accordingly, the U. S. Government retains a nonexclusive, royalty-free license to publish or reproduce the published form of this contribution, or allow others to do so, for U. S. Government purposes.

MASTER

The octupole deformation or octupole vibration is produced by the long range octupole-octupole correlations. These correlations depend on the $r^3Y_3 \cdot r^3Y_3$ matrix elements between single particle states with $\Delta l = \Delta j = 3$ and the energy difference between them. A look at the shell states (Fig. 1) indicates that valence neutrons in the $N \sim 134$ nuclei occupy the $j_{15/2}$ and $g_{9/2}$ orbitals and valence protons in the $Z \sim 88$ nuclei occupy the $i_{13/2}$ and $f_{7/2}$ orbitals. Thus in nuclei with $N \sim 134$ and $Z \sim 88$, both neutrons and protons will have maximum octupole correlations. This mass region is therefore most likely to exhibit octupole deformation. Experimentally, one observes that the energies of the $K, I^\pi = 0, 1^-$ states in the mass 224 nuclei decrease [4] as one goes from ^{228}Th to ^{222}Th indicating that octupole correlations are increasing. Alpha decay hindrance factors show a similar behavior.

Interest in octupole shape was revived in early eighties because of two observations. First, the mass formula [5], which reproduced the experimental masses well in all other regions, predicted less binding in the mass 224 region. Inclusion of small octupole deformation (β_3) in the potential improved the fit. This pointed out large octupole-octupole correlations or deformation in the mass 224 region. Another observation was the presence of the low-lying 0^+ state in ^{234}U , observed in the (p,t) reaction [6], which could not be explained on the basis of the vibrational model. Chasman [7] found that the lowering of the 0^+ state in ^{234}U could be accounted for, if one includes octupole-octupole correlations in the potential. When this calculational technique was extended to odd-mass nuclei in the mass 224 region, it predicted [8] parity doublets with large $B(E3)$ values between its members, which are characteristic signature of octupole deformation. The calculations [9] for the actinides indicate that the additional binding energy due to the β_3 deformation is only ~ 1 MeV, compared with the binding energy of ~ 10 MeV due to the quadrupole deformation (Fig. 2).

It is well known that the rotation of symmetric and asymmetric molecules generate different rotational bands. In the case of the former, the band has 0^+ , 2^+ , 4^+ -- level sequence and the latter has 0^+ , 1^- , 2^+ , 3^- , -- sequence. Thus the rotation of reflection symmetric and reflection asymmetric nuclei will produce different spectra and these can be used as signature of octupole shape. Many spheroidal nuclei are known to show 0^+ , 2^+ , 4^+ level sequence in their ground states but no one has observed the 0^+ , 1^- , 2^+ , 3^- level sequence in any nucleus. Thus it can be safely said that there is no even-even reflection asymmetric nucleus in the ground state. It turns out that the octupole-octupole correlations in nuclei can be enhanced either by rotating the nucleus or by placing an unpaired nucleon in the system. Signature of reflection asymmetry in an odd mass nucleus is the presence of a parity doublet (see Fig. 3) -- a pair of almost degenerate states with the same spin, opposite parity, and connected by a large $B(E3)$ value. Octupole deformations were soon observed both in odd mass nuclei [10] as well as in even-even nuclei at moderate spins [11].

12.2 OCTUPOLE DEFORMATION THE ACTINIDE REGION

In odd mass nuclei, the two members of the parity doublet have very similar wave functions except the parity. Thus one would expect similar properties for both bands. The data on odd mass nuclei in the mass 224 region can be summarized as follows:

1. Parity doublets have been observed in several odd-mass Ra, Ac and Pa nuclei [12-15]. An example [14] is shown in Fig. 4.
2. The members of the doublets are connected by fast E1 transitions [15]. The $B(E1)$ values in these nuclei are larger than 1.0×10^{-3} Weisskopf units (see Fig. 5).

3. Alpha decay rates are enhanced to the parity doublet partner of the favored band.
4. Coriolis matrix elements and M1 transition rates are attenuated.
5. Octupole deformation has also been found at moderate spins [16] in ^{221}Th and ^{223}Th .

In even-even nuclei, levels with alternating parity have been observed in several Ra and Th nuclei. In general, these are connected by fast E1 transitions.

12.3 OCTUPOLE DEFORMATION IN $N \sim 88$, $Z \sim 56$ NUCLEI

As shown in Fig. 1, octupole correlations are also expected in the $Z \sim 56$, $N \sim 88$ nuclei. However, in these nuclei, spacings for the $\Delta L = 3$, $\Delta j = 3$ levels are larger than in the mass 224 region. Hence one expects smaller octupole-octupole correlations than in the mass 224 region. Calculations by Nazarewicz et al. [17] predicted octupole minima for ^{144}B and ^{146}Ba ground states. Later mean field calculations [18] show that the octupole shape stabilizes with rotation.

The nuclei with $Z \sim 56$, $N \sim 88$ are neutron rich and are difficult to access for usual in-beam gamma ray spectroscopy. These nuclei are copiously produced in the spontaneous fission. There are only two conveniently available spontaneous fission sources, ^{252}Cf ($T_{1/2} = 2.646$ y, fission branching = 3.09%) and ^{248}Cm (3.4×10^5 y, fission branching = 8.26%). The mass distributions [19,20] of these nuclei along with that for the 60.5-d ^{254}Cf (fission = 99.7%) [Ref. 21] are shown in Fig. 6.

12.4 EXPERIMENTAL PROCEDURE

Level structures of ^{252}Cf and ^{248}Cm were studied in two experiments carried out with the Argonne Notre Dame BGO gamma ray facility. In the first experiment, a 60 microcurie source (which corresponds to 2 microcurie of fission) embedded in a beryllium cylinder was used and the detector system consisted of 7 Compton suppressed Ge detectors, one low energy photon spectrometer (LEPS) and 14 BGO hexagons. Data were collected for a period of three days. In the experiment performed this year in May, a 5 mg ^{248}Cm source was used and the gamma ray facility consisted of 10 Compton suppressed Ge detectors, two LEPS, and 50 BGO hexagons (see Fig. 7). The Cm source was prepared by mixing curium oxide with 150 mg of KCl and pressing it under a pressure of 124 MPa to make a pellet. The curium was chemically separated from fission products and other actinides just before the preparation of the source. This kind of source was required in order to measure low-energy γ -rays and K X rays, and to stop the fission fragments as soon as they were emitted to avoid Doppler broadening of γ -ray peaks. Spectra were collected for a period of 10 days. In both cases, events were recorded when two Ge's (LEPS) and at least one of the hexagons fired. These triple coincidence events were collected in the event by event mode on magnetic tapes and were later sorted with appropriate gates.

12.5 RESULTS

Gamma ray transitions observed in gated spectra were assigned to nuclides on the following basis:

- 1) In many nuclei, the $2^+ \rightarrow 0^+$ transitions are known from the early Berkeley work [22]. Thus the spectrum gated by the $2^+ \rightarrow 0^+$ γ -ray in

^{144}Ba will contain all ^{144}Ba γ -rays plus those in the complementary Zr isotopes. Next, gating on the Zr transitions, one would be able to distinguish which γ -rays belong to ^{144}Ba .

- 2) In cases where no transition is known in a nucleus, one can identify the nucleus by measuring the γ -ray yield in coincidence with the transitions in the complementary fission product. This has been done for ^{142}Xe (see Fig. 8). From the yield distribution one can determine which transition belongs to ^{142}Xe .
- 3) The multipolarities of strong transitions were deduced from the measured angular correlations. In some cases, the conversion coefficients of the low-energy transitions were deduced from the measured K X' ray intensities. The Ge detectors were sensitive only to γ -rays above 150 keV because the constant fraction discriminator was used in the slow rise time reject mode. For energies below ~ 150 keV, the two LEPS were useful.

Gamma ray spectra were generated for many nuclides by placing appropriate gates. Because of the Compton suppression, the spectra were extremely clean. The sensitivity of the measurement was good enough to observe γ -rays with intensities greater than 1.0% for high-yield fission products. Examples of γ -ray spectra are shown in Fig. 9.

12.6 DISCUSSION

From the analysis of the present data, level schemes of many nuclei around mass 100 and mass 144 were deduced. Level schemes of ^{144}Ba and ^{142}Xe are displayed

in Fig. 10. As can be seen, the levels in ^{144}Ba above $7\hbar$ have alternating parities, indicative of a single rotational band. On the other hand no negative parity band has been observed in ^{142}Xe , suggesting lack of strong octupole correlation in this nucleus. Our results indicate presence of octupole deformation [23,24] in ^{144}Ba , ^{146}Ba and ^{146}Ce above spin $7\hbar$; ^{142}Ba , ^{148}Ce , ^{150}Ce and ^{142}Xe do not exhibit the intertwined negative and positive parity levels. In the case of octupole limit, the positive and negative parity levels constitute a single rotational band with one value of moment of inertia. How well the levels merge to octupole limit can be judged from a plot of δE against the spin, where δE is the difference between the observed energy of a negative parity state and the energy calculated from the energies of the neighboring positive parity states. The quantity δE can be calculated with the expression

$$\delta E = E_{I^-} - \frac{(I+1) \cdot E_{(I-1)^+} + I \cdot E_{(I+1)^+}}{(2I+1)} .$$

For an ideal octupole nucleus, δE (or $\delta E/B$, where B is the rotational constant) should be zero. In Fig. 11, the values of $\delta E/B$ are plotted against spin I for the nuclei studied in the present work and for ^{222}Th and ^{224}Th [11,25]. As can be seen in the figure, δE is quite high at low spin but it decreases as the spin increases and is near zero at $8-9\hbar$, indicating increase of octupole correlations with rotation and stabilization of octupole deformation above spin $8\hbar$.

Another characteristic feature of the octupole shape is the enhancement in the $E1$ transition rates. We have determined the $B(E1)/B(E2)$ ratios for Ba and Ce isotopes. Using the experimentally measured values of the quadrupole moment from the lifetime of $2^+ \rightarrow 0^+$ states [26] and assuming that they do not change

with spin, we have deduced the $B(E1)$ values. These $B(E1)$ values are related to the electric dipole moment D_0 by the following expression

$$B(E1) = 3D_0^2 \langle I_i 010 | I_f 0 \rangle^2 / 4\pi .$$

The dipole moments thus determined are given in table 1. Also included are experimental values for $^{146,148}\text{Nd}$ [27] and ^{150}Sm [28].

Electric dipole moments have been calculated by Leander et al. [29] for the nuclei in the mass 224 region. It has been pointed out by Bohr and Mottelson [30], and Strutinski [31] that a nucleus with reflection asymmetric shape will have an electric dipole moment in the intrinsic reference frame. Only liquid drop contributions were considered by these authors. Leander et al. [29] have calculated the dipole moment by adding the contributions from the liquid drop term as well as shell correction terms. Thus the dipole moment can be written as

$$D_0 = D_{LD} + D_{SC} .$$

The shell correction term contains a term due to neutrons and a term due to protons. These terms were determined by considering the orbits occupied by the nucleons and calculating the displacement of the center of charge from the average position. Leander et al. normalized their calculations to the experimental dipole moment of ^{222}Th and found a good agreement for other nuclei in the mass 224 region. Soon after, Dorso et al. [32] showed that the inclusion of the neutron skin effect (which was ignored by Leander et al.) makes the liquid drop term much smaller and hence the agreement worse.

The calculational technique used by Leander et al was used by Nazarewicz [18] to calculate the dipole moment of nuclei in the mass 144 region. In this calculation, the liquid drop term was not included. The dipole moments calculated only on the basis of the shell correction term are included in table 1 and these are in fair agreement with the experimental data.

12.7 CONCLUSION

Experimental data show that there is no even-even nucleus with a reflection asymmetric shape in its ground state. Maximum octupole-octupole correlations occur in nuclei in the mass 224 ($N \sim 134$, $Z \sim 88$) region. Parity doublets, which are the characteristic signature of octupole deformation, have been observed in several odd mass Ra, Ac and Pa nuclei. Intertwined negative and positive parity levels have been observed in several even-even Ra and Th nuclei above spin $\sim 8\hbar$. In both cases, the opposite parity states are connected by fast E1 transitions. In some medium-mass nuclei intertwined negative and positive parity levels have also been observed above spin $\sim 7\hbar$. The nuclei which exhibit octupole deformation in this mass region are ^{144}Ba , ^{146}Ba and ^{146}Ce ; ^{142}Ba , ^{148}Ce , ^{150}Ce and ^{142}Xe do not show these characteristics. No case of parity doublet has been observed in the mass 144 region.

Acknowledgment: This work was supported by the U.S. Department of Energy, Nuclear Physics Division, under contract No. W-31-109-ENG-38, by the Science and Engineering Research Council of the U.K. and by the National Science Foundation Grant No. PHY-84-16025. The authors are also indebted for the use of ^{248}Cm to the Office of Basic Energy Sciences, U.S. Department of Energy, through the transplutonium element production facilities at the Oak Ridge National Laboratory. Helpful discussions with R. R. Chasman are also acknowledged.

REFERENCES

1. A. Bohr, "The Coupling of Nuclear Surface Oscillations to The Motion of Individual Nucleons", K. Danske Vidensk. Selsk. Mat.-Fys. Medd. 26 (1952) No. 14.
2. A. Bohr and B. R. Mottelson, "Collective and Individual Aspects of Nuclear Structure", K. Danske Vidensk Selsk. Mat.-Fys. Medd. 27 (1953) No. 16.
3. F. S. Stephens, F. Asaro and I. Perlman, "Low-Lying 1^- States in Even-Even Nuclei", Phys. Rev. 96 (1954) 1568; "Radiations from 1^- States in Even-Even Nuclei", Phys. Rev. 100 (1955) 1543.
4. C. M. Ledere and V. S. Shirley, "Table of Isotopes", John Wiley, Inc., New York, 7th ed. 1978.
5. P. Möller and J. R. Nix, "Nuclear Mass Formula with a Yukawa-Plus-Exponential Macroscopic Model and a Folded-Yukawa Single-Particle Potential", Nucl. Phys. A361 (1981) 117.
6. J. A. Maher, J. R. Erskine, A. M. Friedman, R. H. Siemssen and J. P. Schiffer, "Population of 0^+ States in Actinide and $A \sim 190$ Nuclides by the (p,t) Reaction", Phys. Rev. C5 (1972) 1380.
7. R. R. Chasman, "Octupole-Octupole Residual Interactions and Low-Lying 0^+ Excited States in the Isotopes ^{232}U , ^{234}U , and ^{236}U ", Phys. Rev. Lett. 42 (1979) 630.
8. R. R. Chasman, "Incipient Octupole Deformation and Parity Doublets in the Odd Mass Light Actinides", Phys. Lett. 96B (1980) 7.
9. R. R. Chasman, "Octupole Correlations in the Heavy Elements", Nuclear Structure, Reactions and Symmetries, edited by R. A. Meyer and V. Paar, World Scientific Co. Singapore, 1986.

10. I. Ahmad, J. E. Gindler, R. R. Betts, R. R. Chasman and A. M. Friedman, "Possible Ground-State Octupole Deformation in ^{229}Pa ", Phys. Rev. Lett. 49 (1982) 1758.
11. D. Ward, G. D. Dracoulis, J. R. Leigh, R. J. Charity, D. J. Hinde and J. O. Newton, "High Spin states in ^{222}Th ", Nucl. Phys. A406 (1983) 591.
12. R. K. Sheline and G. A. Leander, "Strong and Weak Coupling to the Octupole-Deformed Mode in ^{227}Ac ", Phys. Rev. Lett. 51 (1983) 359.
13. G. A. Leander and Y. S. Chen, "Reflection-Asymmetric Rotor Model of Odd $A\sim 219-229$ Nuclei", Phys. Rev. C37 (1988) 2744.
14. I. Ahmad, J. E. Gindler, A. M. Friedman, R. R. Chasman and T. Ishii, "Level Structure of ^{225}Ac ", Nucl. Phys. A472 (1987) 285.
15. I. Ahmad, R. Holzmann, R. V. F. Janssens, P. Dendooven, M. Huyse, G. Reusen, J. Wauters and P. Van Duppen, "Octupole Deformation in ^{223}Ac ", Nucl. Phys., in press.
16. M. Dahlinger, E. Kankeleit, D. Habs, D. Schwalm, B. Schwartz, R. S. Simon, J. D. Burrows and P. A. Butler, "Alternating Parity Bands and Octupole Effects in ^{221}Th and ^{223}Th ", Nucl. Phys. A484 (1988) 337.
17. W. Nazarewicz, P. Olanders, I. Ragnarsson, J. Dudek, G. A. Leander, P. Möller, and E. Ruchowska, "Analysis of Octupole Instability in Medium-Mass and Heavy Nuclei", Nucl. Phys. A429 (1984) 269.
18. W. Nazarewicz, "Dipole and Octupole Correlations in the $Z\sim 56$, $N\sim 88$ Mass Region", Int. Conf. on Nuclear Structure through Static and Dynamic Moments (Melbourne, Australia) (1987) 180.
19. K. F. Flynn, J. E. Gindler and L. E. Glendenin, "The Mass Distribution for Spontaneous Fission of ^{252}Cf ", J. Inorg. Nucl. Chem. 37 (1975) 881.
20. K. F. Flynn, J. E. Gindler and L. E. Glendenin, "Mass Distributions for the Spontaneous Fission of ^{248}Cm and ^{250}Cf ", J. Inorg. Nucl. Chem. 39 (1977) 759.

21. J. E. Gindler, K. F. Flynn, L. E. Glendenin and R. K. Sjoblom,
"Distribution of Mass, Kinetic Energy, and Neutron Yield in the Spontaneous Fission of ^{254}Fm ", Phys. Rev. C16 (1977) 1483.
22. E. Cheifetz, J. B. Wilhelmy, R. C. Jared and S. G. Thompson, "Determination of the Charge and Mass Distribution in the Fission of ^{252}Cf ", Phys. Rev. C4 (1971) 1913.
23. W. R. Phillips, I. Ahmad, H. Emling, R. Holzmann, R. V. F. Janssens, T. L. Khoo and M. W. Drigert, "Octupole Deformation in Neutron-Rich Ba Isotopes", Phys. Rev. Lett. 57 (1986) 3257.
24. W. R. Phillips, R. V. F. Janssens, I. Ahmad, H. Emling, R. Holzmann, T. L. Khoo and M. W. Drigert, "Octupole Correlation Effects Near $Z=56$, $N=88$ ", Phys. Lett. 212 (1988) 402.
25. P. Shuler et al., "High Spin States in $^{224,226,228}\text{Th}$ and the Systematics of Octupole Effects in Even Th Nuclei", Phys. Lett. 174B (1986) 241.
26. G. Mamane, E. Cheifetz, E. Dafni, A. Zemel and J. B. Wilhelmy, "Lifetime Measurements of Excited Levels in Prompt Fission Products of ^{252}Cf ", Nucl. Phys. A454 (1986) 213.
27. W. Urban, R. M. Lieder, W. Gast, G. Hebbinghaus, A. Kramer-Flecken, T. Morek, T. Rzaca-Urban, W. Nazarewicz and S. L. Tabor, "Octupole Instability Induced by Rotation in the Nuclei $^{146,148}\text{Nd}$ ", Phys. Lett. 200B (1988) 424.
28. W. Urban, R. M. Lieder, W. Gast, G. Hebbinghaus, A. Kramer-Flecken, K. P. Blume and H. Hubel, "Evidence for Coexistence of Reflection Asymmetric and Symmetric Shapes in ^{150}Sm ", Phys. Lett. 185B (1987) 331.
29. G. A. Leander, W. Nazarewicz, G. F. Bertsch and J. Dudek, "Low-Energy Collective E1 Mode in Nuclei", Nucl. Phys. A453 (1986) 58.
30. A. Bohr and B. R. Mottelson, "Electric Dipole Moment Associated with Octupole Vibrations of a Spheroidal Nucleus", Nucl. Phys. 4 (1957) 529.

31. V. M. Strutinskii, "Remarks on Mirror-Asymmetrical Nuclei", Atomnaya Energiya 4 (1956) 150; Atomic Energy (USSR) 4 (1956) 164.
32. C. O. Dorso, W. D. Myers and W. J. Swiatecki, "Droplet-Model Electric Dipole Moments", Nucl. Phys. A451 (1986) 189.

Table 1. Experimental and Theoretical Intrinsic
Electric Dipole Moments

Nucleus	D_0 (exp)	D_0 (theory)
	e fm	e fm
^{142}Xe	--	0.02
^{144}Ba	0.13 ± 0.01	0.09
^{146}Ba	0.04 ± 0.01	0.03
^{144}Ce	0.17 ± 0.05	0.16
^{146}Ce	0.16 ± 0.04	0.18
$^{146}\text{Nd}^a$	0.18 ± 0.01	0.20
$^{148}\text{Nd}^a$	0.23 ± 0.03	0.22
$^{150}\text{Sm}^a$	0.20 ± 0.01	0.25

^aValues for these nuclei are taken from Refs. 27 and 28.

Figure Captions

- Fig. 1. Shell model states for neutrons showing the locations where states with $\Delta j = 3$ occur in nuclei.
- Fig. 2. Calculated increase in binding energy as a function of quadrupole deformation β_2 and octupole deformation β_3 for an actinide nucleus.
- Fig. 3. Signatures of reflection asymmetry in even-even and odd mass nuclei.
- Fig. 4. Level scheme of ^{225}Ac deduced from the study of ^{229}Pa alpha decay. Two parity doublets $5/2^\pm$ and $3/2^\pm$ were identified.
- Fig. 5. El rates in odd mass actinides. Plotted are the ratios of experimental $B(\text{El})$ values and Weisskopf estimates. Weisskopf estimate ($T_{\text{w.u.}}$) was calculated from the formula $T_{\text{w.u.}} = 1.0 \times 10^{14} \cdot A^{2/3} \cdot E_\gamma^3$, where A is the mass number and E_γ is the γ -ray energy in MeV.
- Fig. 6. Fission yields for ^{248}Cm , ^{252}Cf , and ^{254}Cf determined by radiochemical methods.
- Fig. 7. Argonne Notre Dame Gamma Ray Facility used in the experiments described here. For the present experiment, two 90° Ge detectors were removed. A $2 \text{ cm}^2 \times 1 \text{ cm}$ LEPS detector was placed at 90° and a $5 \text{ cm}^2 \times 1 \text{ cm}$ LEPS detector was placed at 0° .
- Fig. 8. Distribution of γ -ray yield against various Mo isotopes
- Fig. 9. Samples of coincidence spectra for ^{144}Ba and ^{142}Xe .
- Fig. 10. Partial level schemes for ^{144}Ba and ^{142}Xe deduced from the present study.
- Fig. 11. A plot of the energy differences ($\delta E/B$) versus spin I for levels in ^{144}Ba , ^{146}Ba , ^{146}Ce , ^{222}Th and ^{224}Th . The data for ^{146}Ba are almost indistinguishable from those for ^{144}Ba and are known up to spin $9\hbar$. $\delta E/B$ is defined in the text. Data on ^{222}Th and ^{224}Th are taken from Ref. 11 and 25.

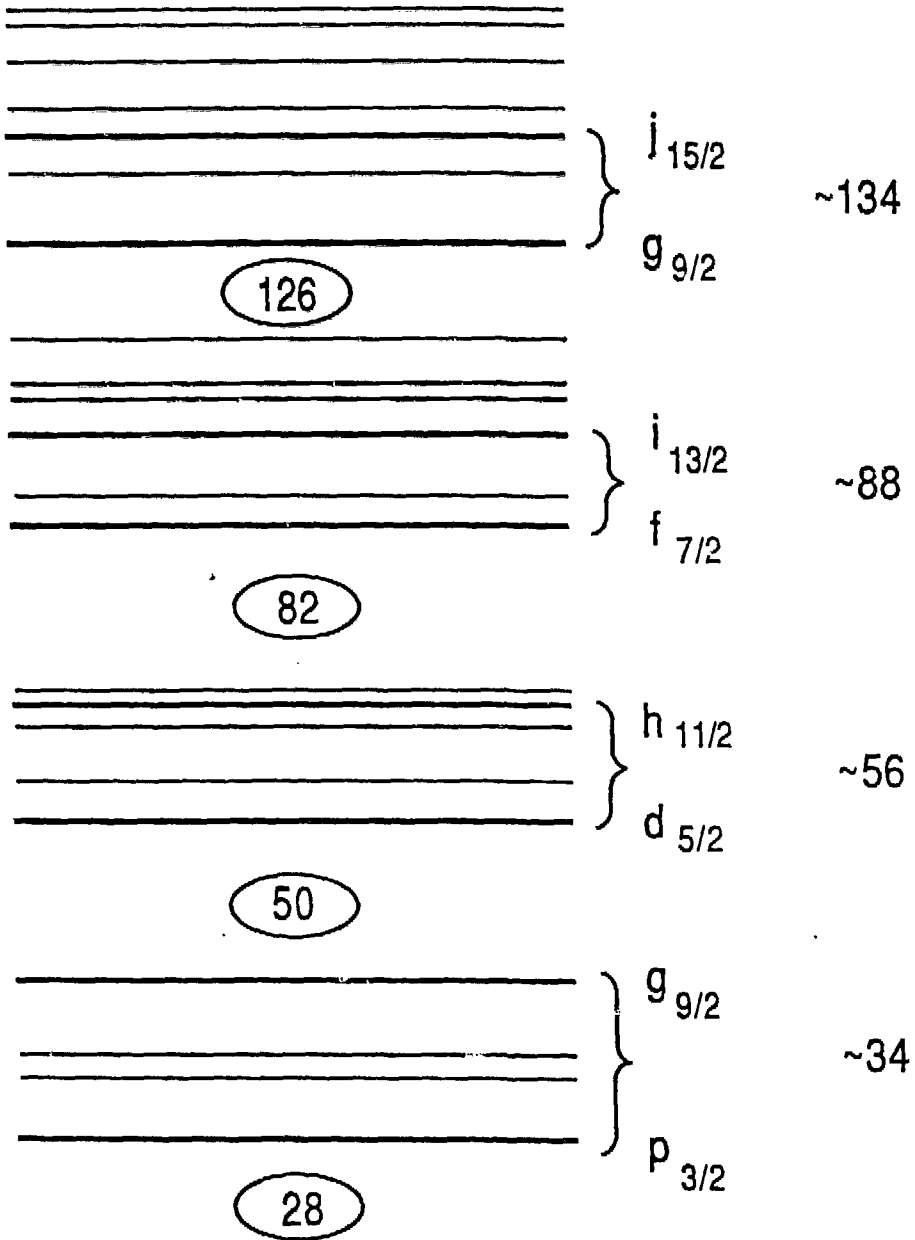
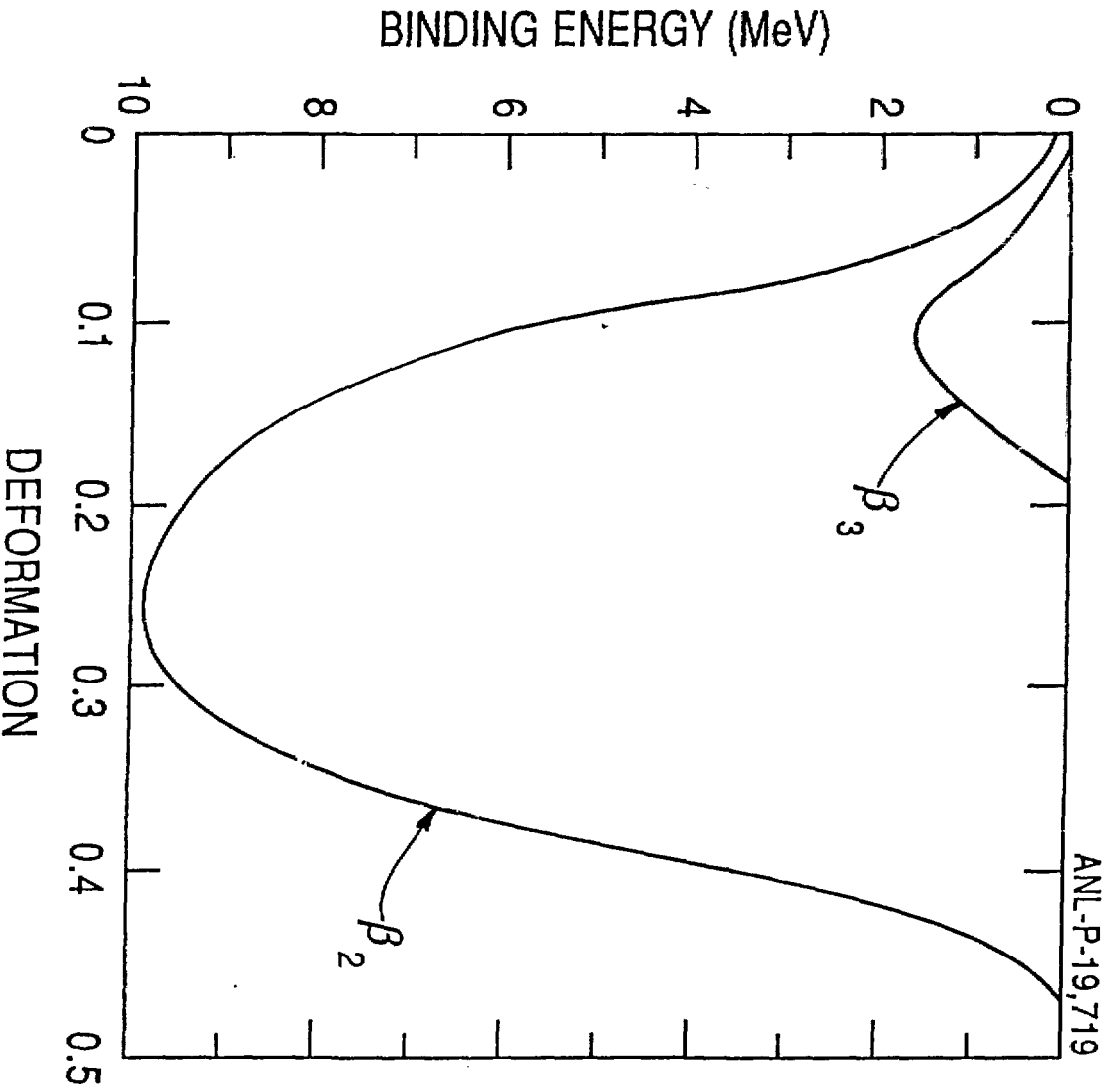
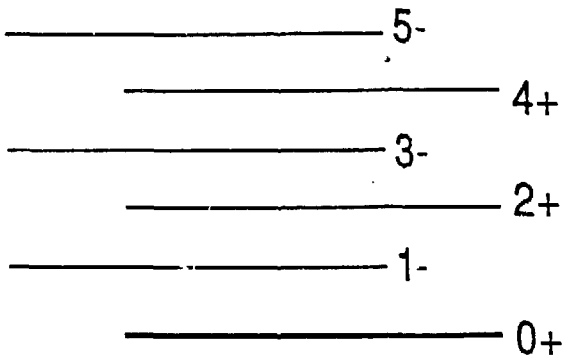
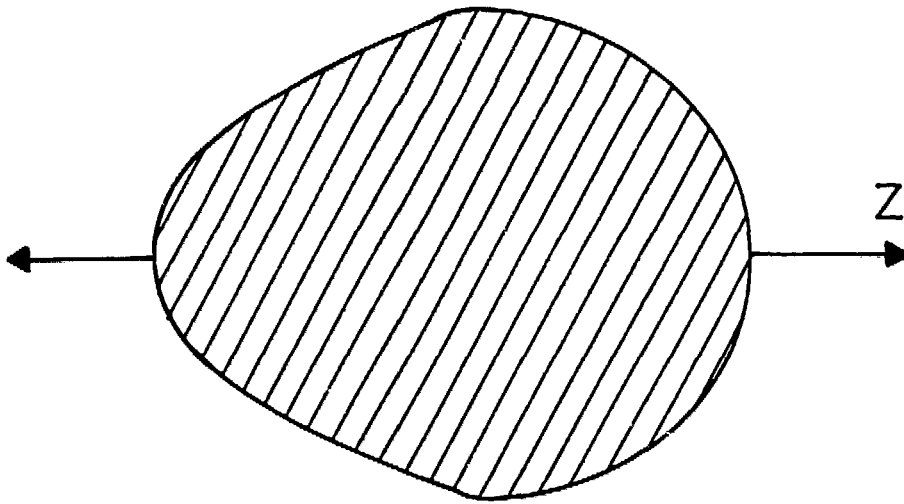


Fig. 1

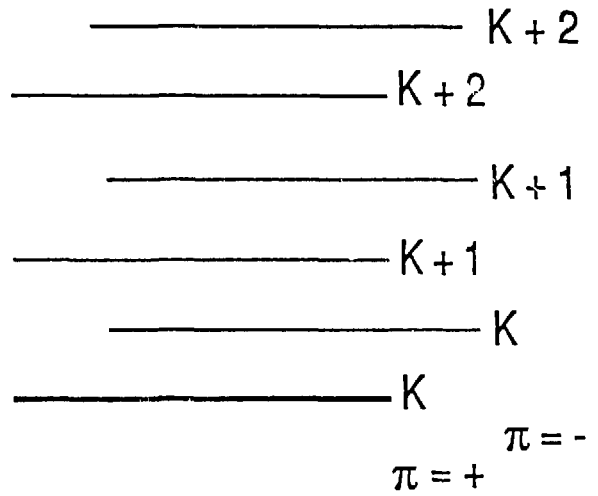


ANL-P-19,719

Fig. 2

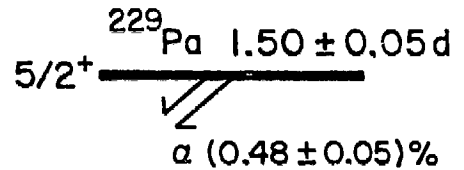
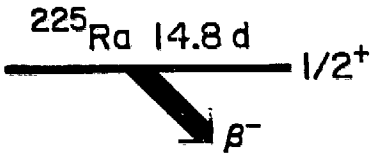


EVEN - EVEN
NUCLEUS



ODD - MASS
NUCLEUS

Fig. 3



log ft, Intensity I^π

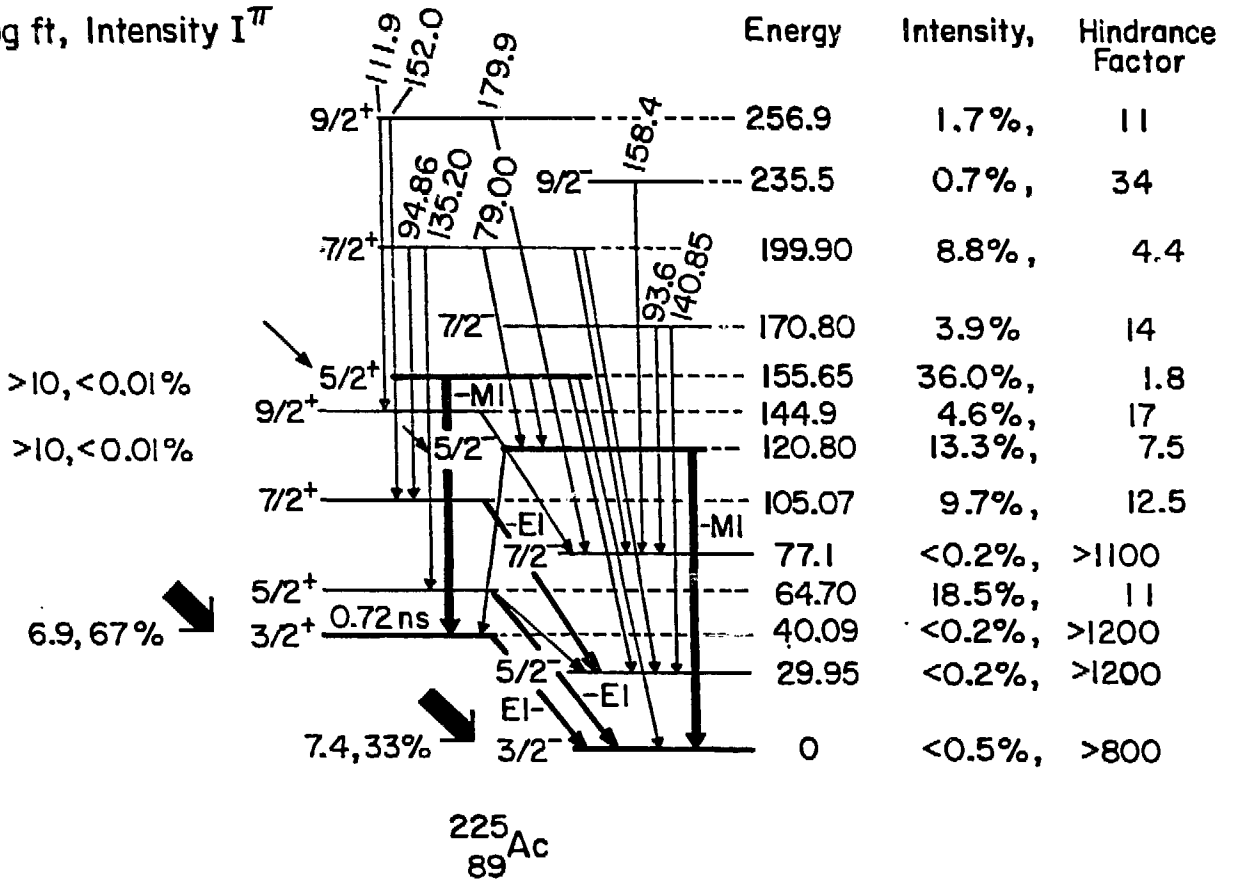


Fig. 4

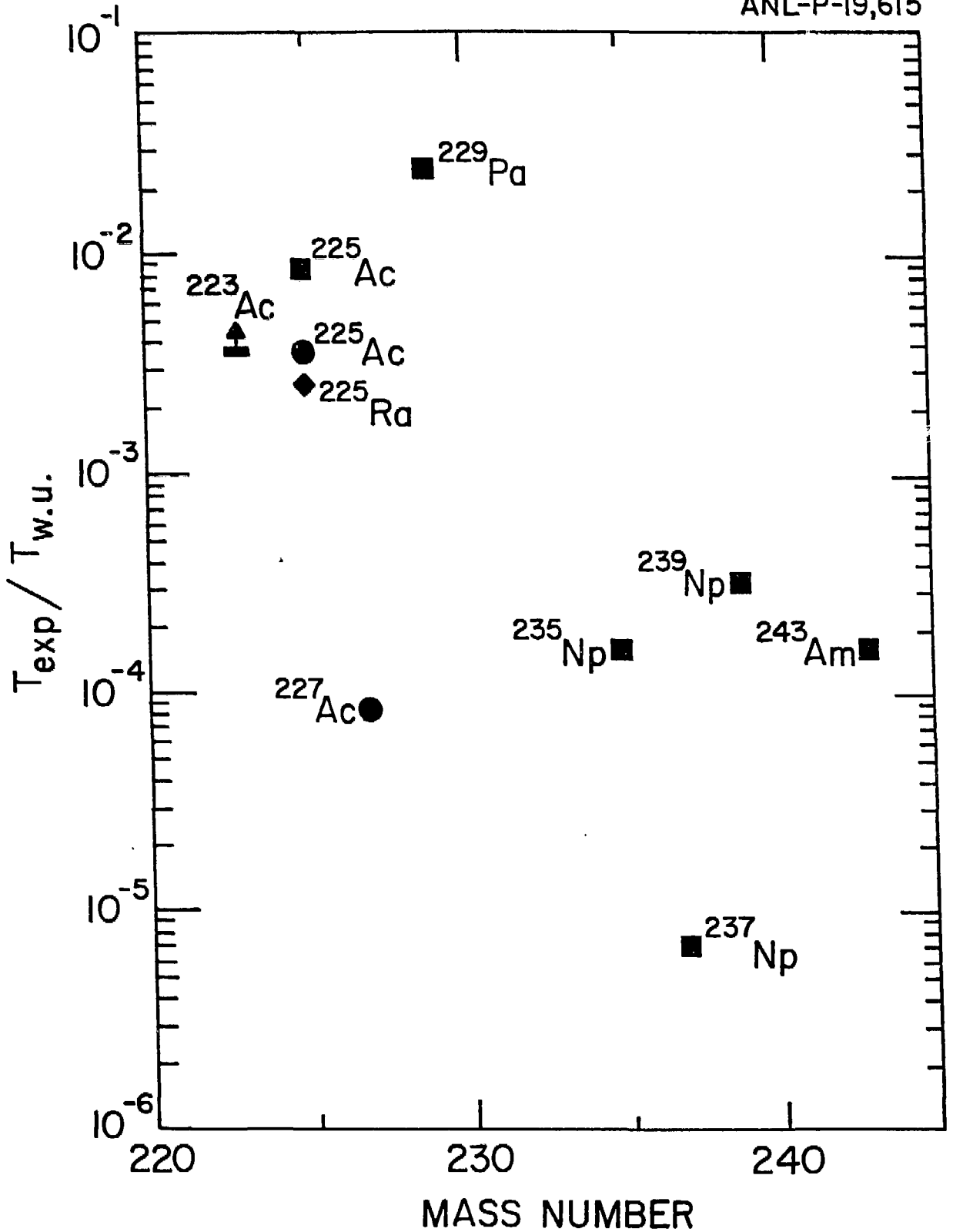


Fig. 5

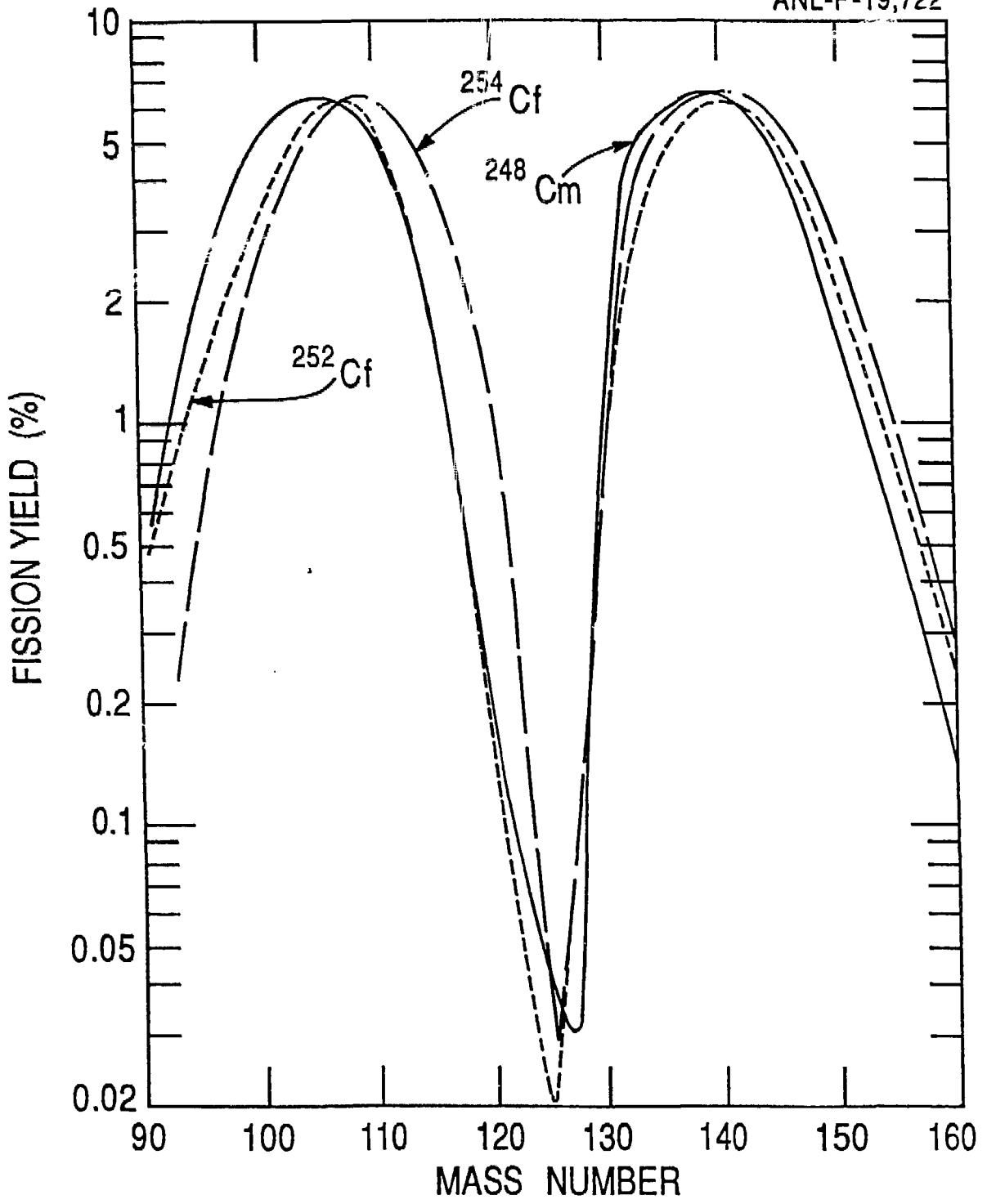


Fig. 6

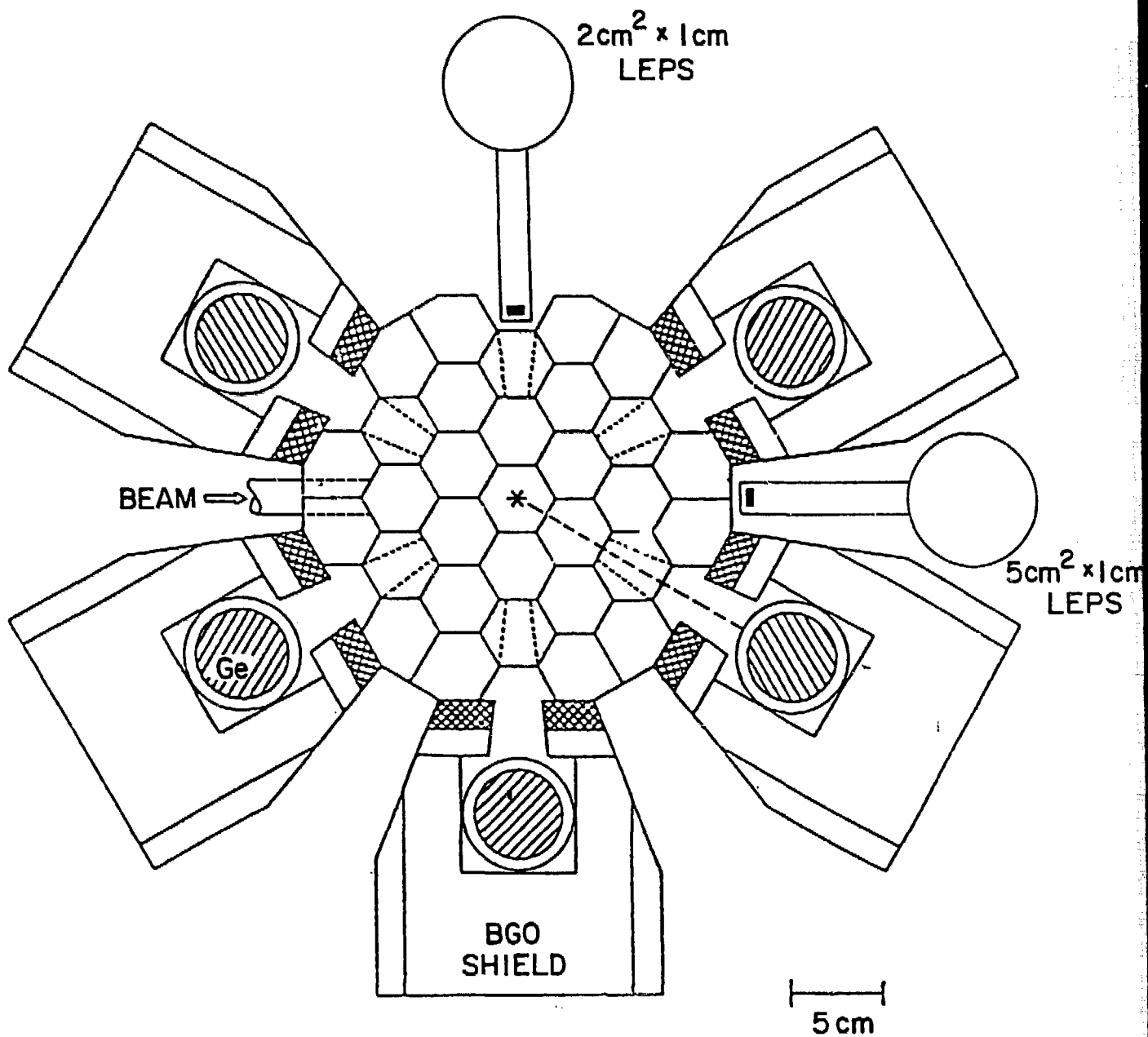


Fig. 7

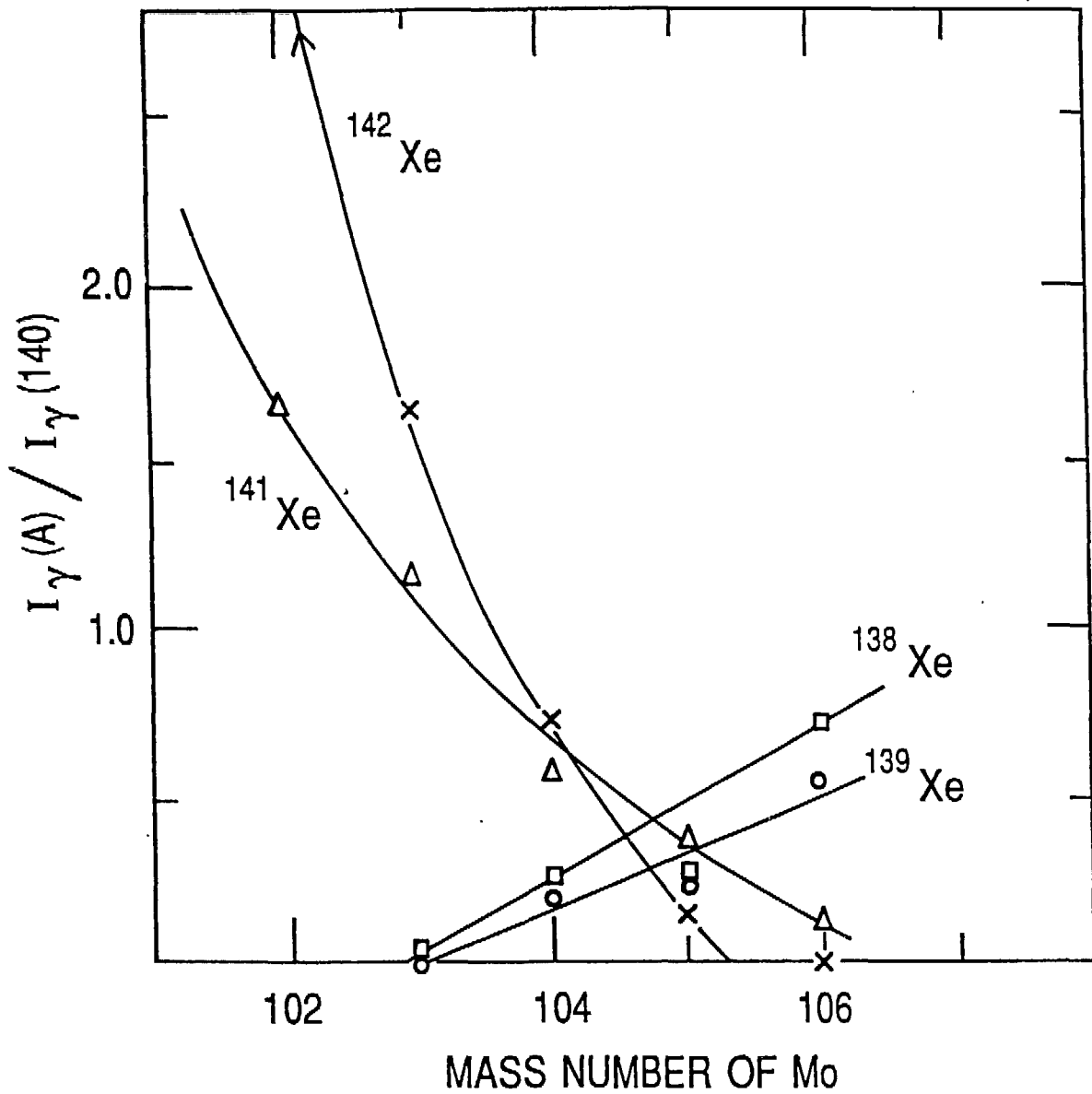


Fig. 8

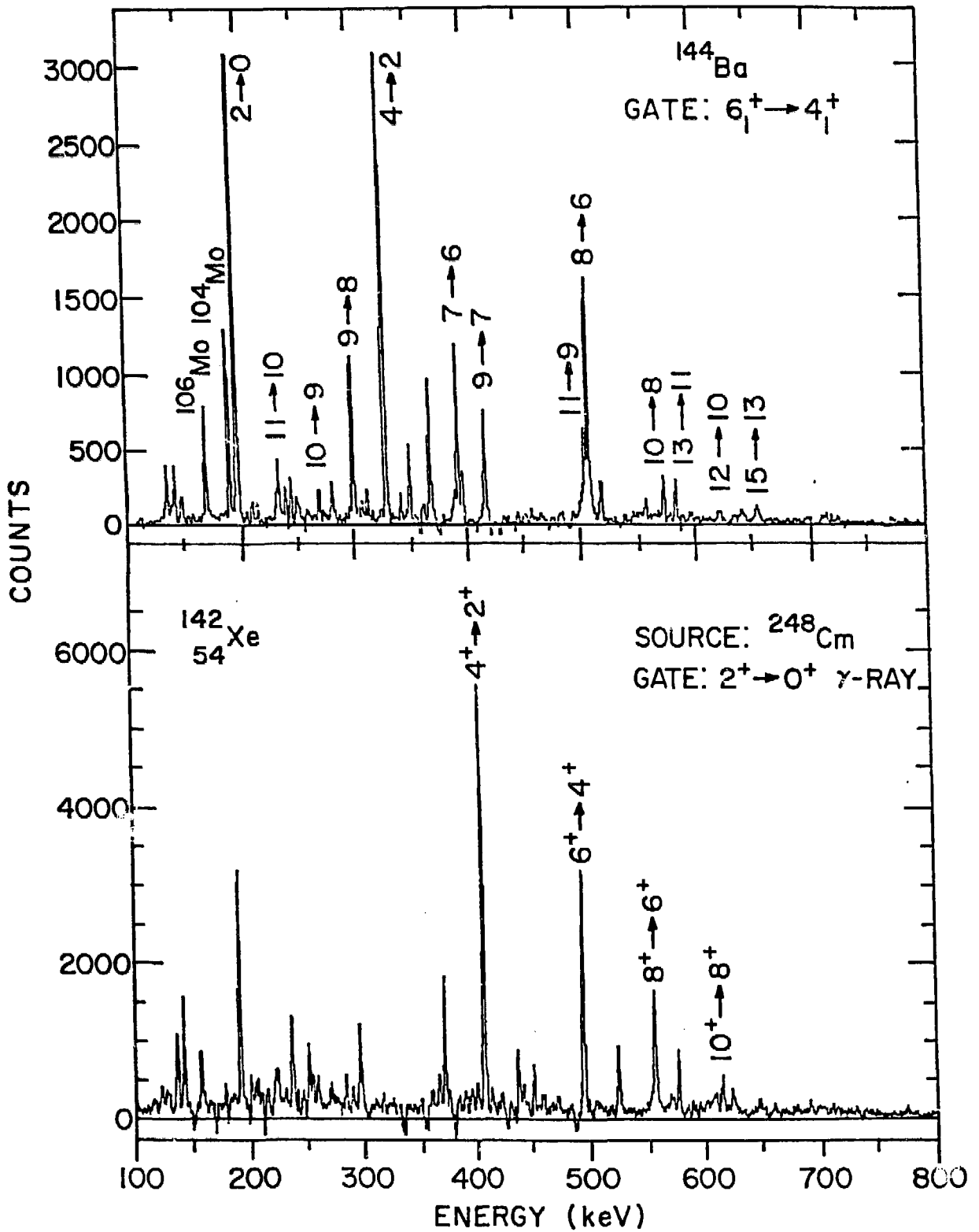


Fig. 9

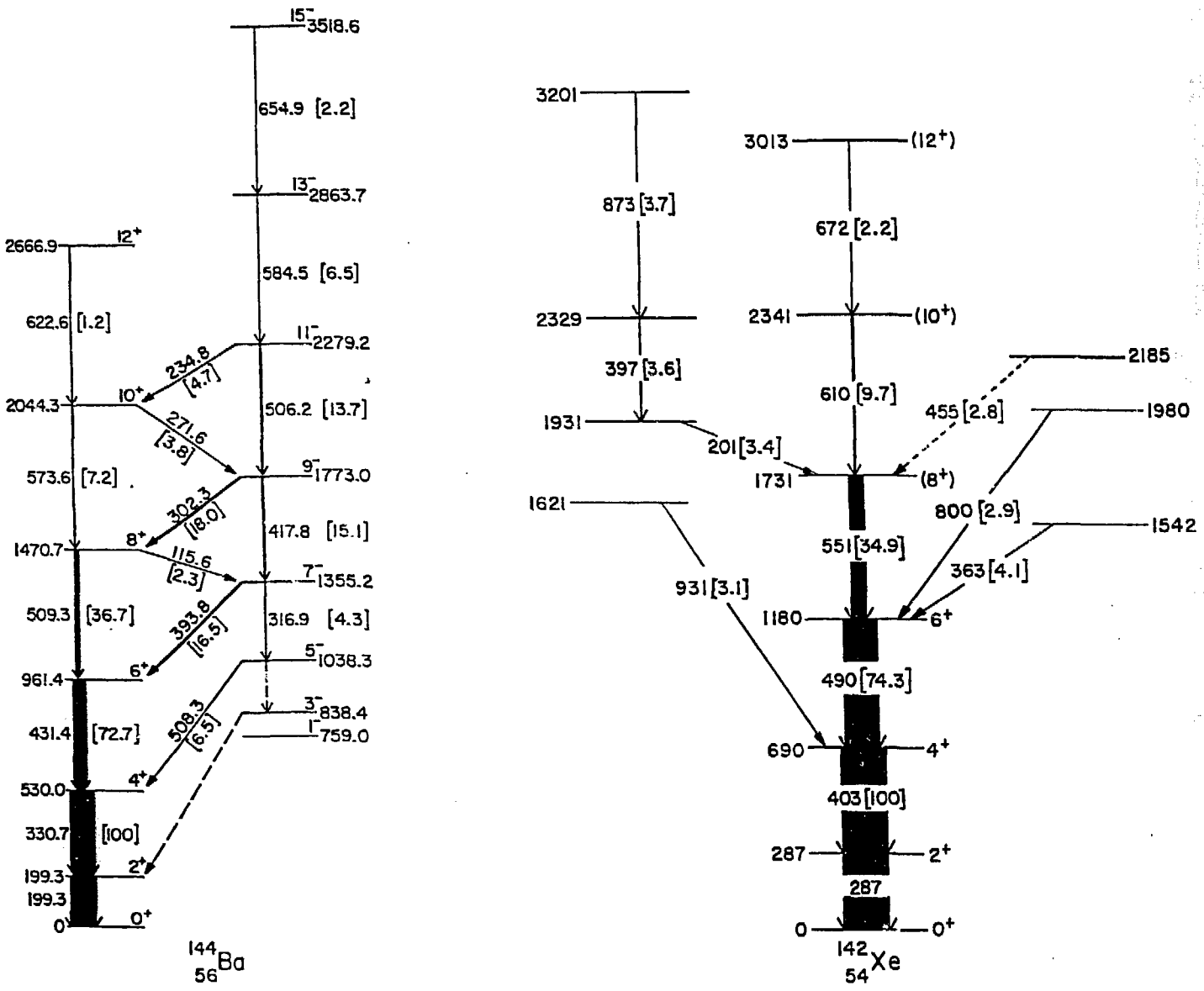
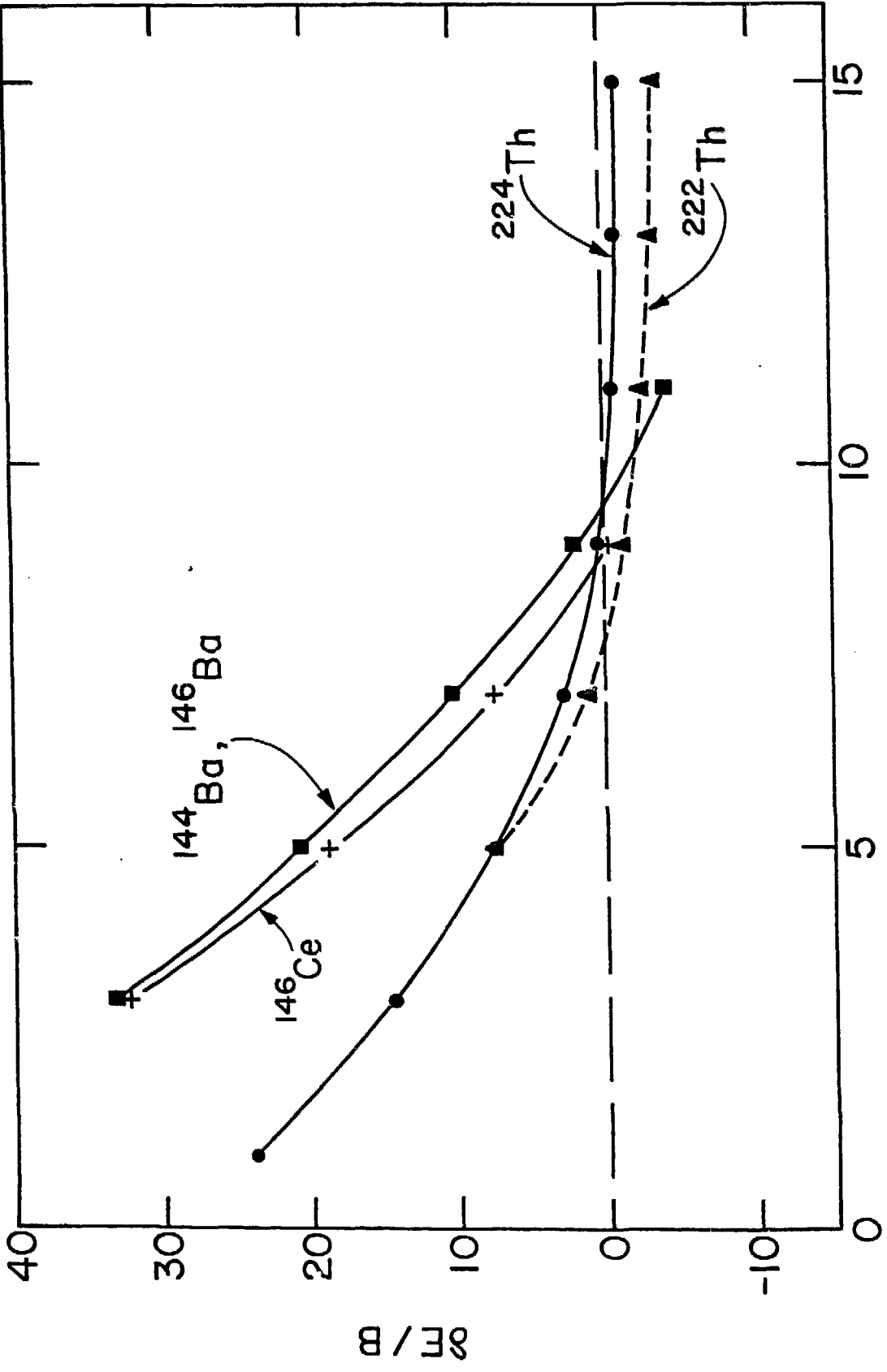


Fig. 10



I

Fig. 11